LAWRENCE
LIVERMORE
NATIONAL
LABORATORY

UCRL-TR-204262-REV-1

Thermal Decomposition Kinetics of HMX

A. K. Burnham, R. K. Weese

November 29, 2004

This work was performed under the auspices of the U.S. Department of Energy by University of California, Lawrence Livermore National Laboratory under Contract W-7405-Eng-48.

Thermal Decomposition Kinetics of HMX

Alan K. Burnham and Randall K. Weese

Lawrence Livermore National Laboratory
P. O. Box 808
Livermore, CA 94551-0808

Abstract

Nucleation-growth kinetic expressions are derived for thermal decomposition of HMX from a variety of thermal analysis data types, including mass loss for isothermal and constant rate heating in an open pan and heat flow for isothermal and constant rate heating in open and closed pans. Conditions are identified in which thermal runaway is small to nonexistent, which typically means temperatures less than 255 ^{o}C and heating rates less than 1 ^{o}C/min. Activation energies are typically in the 140 to 165 kJ/mol range for open pan experiments and about 150 to 165 kJ/mol for sealed pan experiments. Our activation energies tend to be slightly lower than those derived from data supplied by the University of Utah, which we consider the best previous thermal analysis work. The reaction clearly displays more than one process, and most likely three processes, which are most clearly evident in open pan experiments. The reaction is accelerated in closed pan experiments, and one global reaction appears to fit the data well. Comparison of our rate measurements with additional literature sources for open and closed low temperature pyrolysis from Sandia gives a likely activation energy of 165 kJ/mol at 10% conversion.

Keywords: thermal decomposition, chemical kinetics, activation energy, HMX, thermal analysis

1. Introduction

Optimizing the application of high explosives for innumerable applications often employs mechanistic models of the deflagration and detonation processes. Such models usually require an estimation of the amount of gas generated and heat released as a function of time and temperature. Methods for calibrating the gas and heat generation rates range from fitting empirical equations to complex, integrated experiments to detailed mechanistic chemical kinetic models.

Thermal analysis, specifically thermogravimetric analysis (TGA), differential thermal analysis (DTA), and differential scanning calorimetry (DSC), is frequently used as a part of developing global kinetic models of the decomposition process. Unfortunately, the range of experimental results and kinetic parameters from these techniques is so great that some modelers regard such kinetic information with great skepticism, and justifiably so.

The objective of this paper is to obtain meaningful global kinetic models for mass loss and heat generation for the decomposition of HMX. We conclude that the best prior published work in this regard using thermal analysis is that of Wight and Vyazovkin,[1] who took great effort to maintain conditions where thermal runaway of the sample is avoided. We agree with their conclusion that the experiments must be done at relatively

low temperatures or heating rates, that the mean activation energy for HMX decomposition is in the vicinity of 150 kJ/mol, and that it varies with extent of conversion. We also present a comparison to unpublished University of Utah data, collected by Peter Lofy and provided by Prof. Chuck Wight. Activation energies from our data tend to be about slightly lower than from the Utah data, but the difference is small compared to the spread of values in the literature.

Ancillary conclusions of Wight and Vyazovkin are that the best way to derive kinetic parameters is with "model free" isoconversional methods and that model fitting gives unreliable results. We agree with their conclusion in that regard for the subset of data analysis procedures they considered, which are typical for the thermal analysis community. However, we show that model fitting can be a useful approach to analyzing the data when multiple thermal histories are analyzed simultaneously. Comparing behavior for isothermal and linear heating can also give insight into model validity.

In addition, we show that the kinetic parameters for heat release and mass loss are not identical, because they measure different processes, and that the heat release kinetics depend on the nature of the sample confinement, which influences the extent of secondary reactions involving gaseous products.

Finally, we show based on an additional comparison to lower temperature decomposition work by Behrens[2] and Andrzejewski[3] that the global activation energy for HMX decomposition is probably about 165 kJ/mol for a reaction extent of 10%. Although the activation energies from any particular study may be higher or lower, this activation energy fits data from sealed tube experiments at 120 ^{o}C over 5 years to thermal analysis experiment taking a few minutes at temperatures up to 270 ^{o}C.

2. Experimental Methods

2.1. Samples

The β-HMX used in this study (LLNL req. B-844) was manufactured by Holston Defense Corporation (HOL 81H030-033) for Lawrence Livermore National Laboratory using the Bachmann synthesis process. It was determined to be >99.90% pure as analyzed by HPLC for RDX. Particle size analysis indicated that >90% of the material was between 30 and 500 μm in diameter.

2.2. Reaction Measurements

Simultaneous TGA and DTA measurements were carried out using a Simultaneous Differential Thermogravimetric Analyzer (SDT), TA Instruments model 2960. Degradation was carried out under nitrogen carrier gas at a flow rate of 100 cm^3/min. A Differential Scanning Calorimeter (DSC), TA Instrument Model 2920, and its associated software, Universal Analysis, were used for additional analyses. All samples were weighed in a Sartorius MC 5 Electronic balance accurate to ≤ 5 μg. All sample pan total weights were matched with a reference pan of the same mass (or within 100 μg) to match heat flow due to the heat capacity of aluminum for the sample and reference.

For kinetics measurements, sample weights of 0.5 mg or less were decomposed from ~20 ˚C to 350 ˚C at heating rates ranging from 0.1 to 1.0 ^{o}C/min or isothermally at or between 230 and 250 ^{o}C. Figure 1 demonstrates why it is necessary to use such small

samples and slow heating rates. Here, a 2-mg sample was heated at 10 °C/min. During decomposition, the measured sample temperature deviated by more than 10 °C from linearity. When plotted versus temperature, both the temperature difference and the mass showed reversals as the sample cooled just after the main stage of decomposition even as the furnace temperature continued to increase. The maximum temperature excursion was still about 5 °C at 2.5 °C/min but decreased to less than 0.5 °C at 1 °C/min. Decreasing the sample size to less than 0.5 mg ensured that the temperature error was negligible and that the decomposition occurred from the solid state.

Another problem at high heating rates is that the melting endotherm at 280-285 °C distorts both the thermal history and the heat flow data as the peak decomposition temperature passes through that regime as heating rate increases from 2.7 to 7.4 °C/min, as shown in Figure 2. The decomposition rate is possibly affected by phase change. In addition, the total amount of heat generated may increase due to increased secondary reactions so that the isoconversional principle is no longer satisfied. Both of these factors support the need to stay below 1 °C/min to determine valid kinetic parameters.

3. Kinetic Analysis

Data were collected and processed so that each experiment had between 100 and 1500 points covering the region over which any reaction occurred. Kinetic analysis was done with the LLNL program Kinetics05, which is an upgrade of a program described earlier [4]. Three principal methods of kinetic analysis were used.

The first is Friedman's method [5]. For an nth-order Arrhenius reaction,

$$\ln(-d(1-\alpha)/dt) = -E/RT + \ln(A(1-\alpha)^n), \quad (1)$$

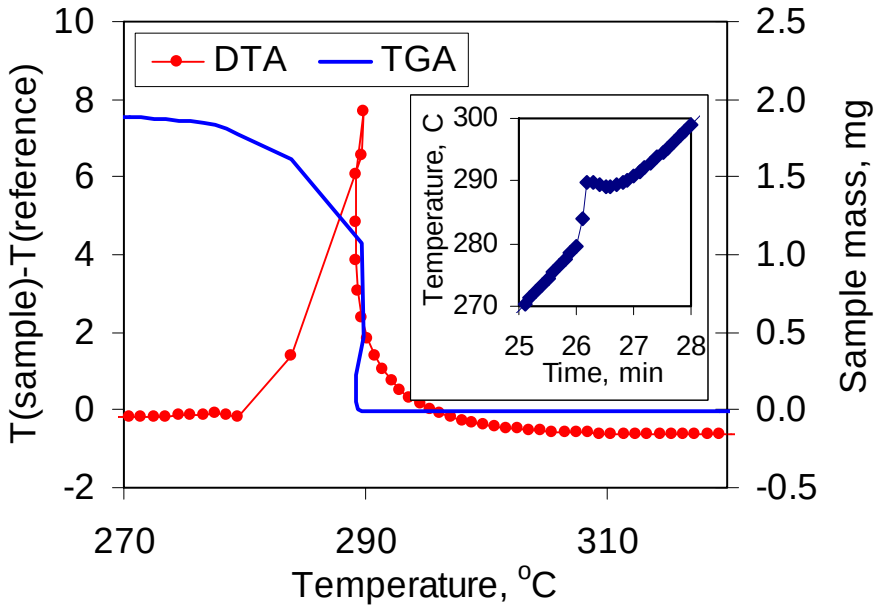

Figure 1. Heat flow and remaining mass for a relatively large sample (2 mg) and rapid heating rate (10 °C/min) showing thermal runaway due to the exothermal reaction. Our kinetics experiments used heating rates less than 1 °C/min and samples less than 0.5 mg.

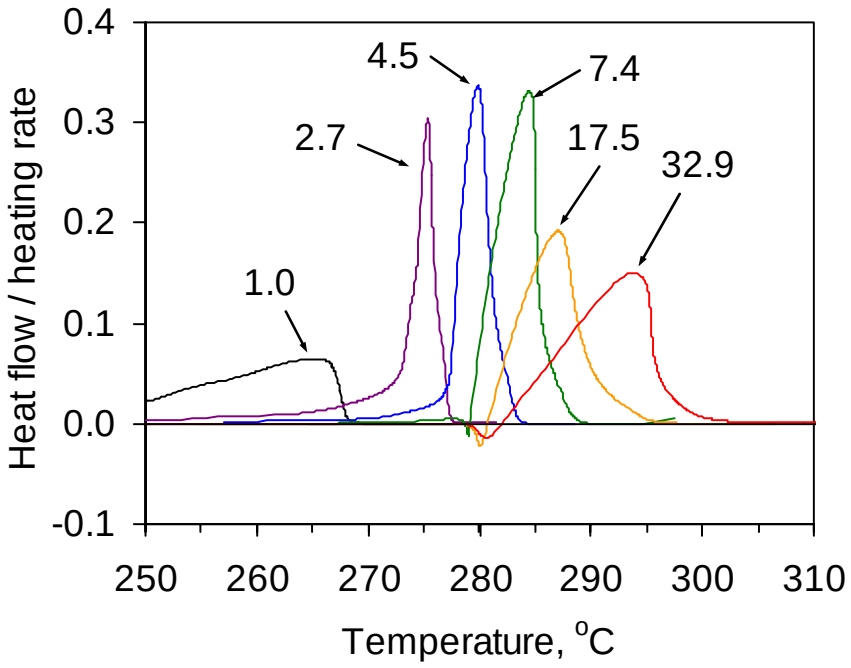

Figure 2. Heat flow normalized to the integrated heat flow and divided by the heating rate for HMX heated in a perforated DSC pan at heating rates from 1.0 to 32.9 °C/min. The endotherms ~280 °C are due to melting, and they shift at higher heating rates due to either kinetic or heat transfer limitations. In this revision, temperatures were corrected by the relation $T_{true} = T_{meas} - H_r/10$ determined by calibration with In and Sn at heating rates from 0.5 to 100 °C/min.

where α is the fraction converted and n is the reaction order. A plot of $\ln(-d(1-\alpha)/dt)$ at a given fraction reacted versus the 1/T value at which that conversion is reached for several different thermal histories will be linear with a slope equal to –E/R and an intercept of $\ln(A(1-\alpha)^n)$.

The second is an extension [2,6] of Kissinger's method [7], where a plot of a function of heating rate and T_{max} versus $1/T_{max}$ gives E/R from the slope and A/E from the intercept:

$$\ln(H_r/RT_{max}^2) = - E/RT_{max} + \ln(A/E) \qquad (2)$$

Our extension looks at the ratio of the measured and calculated profile widths and the profile asymmetry to estimate other reaction parameters such as reaction order and nucleation characteristics.

The third is nonlinear regression to an extended Prout-Tompkins (PT) model [4]:

$$d(1-\alpha)/dt = -k(1-\alpha)^n(1-q(1-\alpha))^m \qquad (3)$$

where m is a nucleation parameter, q is an initiation parameter ordinarily fixed at 0.99, and $k = A\exp(-E/RT)$. The nonlinear regression minimized the squared residuals simultaneously for a chosen criterion. Ordinarily, we weighted each experiment equally and minimized the residuals for both the reaction extent and reaction rate.

4. Results

4.1. Single reaction fits to mass loss

Mass loss provides a measure of both evaporation and formation of volatile products. Table 1 summarizes the rate constants derived for mass loss from an open pan for both constant heating rate and the first set of isothermal conditions. Isoconversional kinetics are determined for the two sets separately and agree qualitatively. The modified Kissinger analysis gives a similar activation and frequency factor and initial estimates for reaction order and nucleation order. Nonlinear regression of both sets separately and together give similar results.

The only definitive way to compare various kinetic expressions is to plot the data and calculations together. In Figure 3, the reactions rates for the isothermal and constant heating rates experiments are compared to their respective fits. The single reaction models fit reasonably well, but there are clear indications of multiple reaction processes. In Figure 4, the fractions reacted for both sets of data are compared with all three sets of nonlinear regression kinetic parameters. The three sets of parameters agree well with each other and the data at the highest temperature and heating rate. The isothermal kinetic parameters become progressively slower than the other two as temperature decreases. This is reflected in the higher activation energy from the isothermal experiments.

Table 1. Kinetic parameters derived from mass loss (open-pan TGA) for both constant heating rate and isothermal heating of HMX at LLNL.

	Constant heating rate			Isothermal		
Friedman	$A_{n=1}$	E	σ_E	$A_{n=1}$	E	σ_E
0.1	9.13E+08	125.5	6.3	1.53E+11	148.8	6.9
0.2	1.80E+11	146.1	0.5	1.44E+11	145.2	29.0
0.3	1.91E+11	145.5	2.0	1.27E+09	123.8	23.8
0.4	7.29E+10	140.6	0.8	3.20E+10	137.0	16.2
0.5	6.39E+10	139.2	1.6	2.27E+12	154.6	11.2
0.6	9.70E+10	140.0	3.1	1.91E+12	153.4	10.0
0.7	2.75E+11	143.7	2.9	3.26E+12	155.3	21.9
0.8	9.07E+11	147.7	2.2	6.97E+12	157.6	5.9
0.9	5.20E+12	153.2	2.6	3.64E+13	162.9	2.7
Kissinger	$A_{n=1}$	E	σ_E	A_{PT}	n	m
(c.h.r. only)	1.30E+10	135.6	3.5	3.54E10	0.649	0.722
Nonlin. Reg. PT	A_{PT}	E	n	m	$T_{50\%}$*	
const. h. r.	1.087E+11	141.4	0.483	0.539	249.9	
isothermal	9.243E+11	148.9	0.901	0.740	252.0	
both	5.501E+10	137.7	0.639	0.647	250.9	

*Calculated temperature for 50% conversion at 0.5 ^{o}C/min

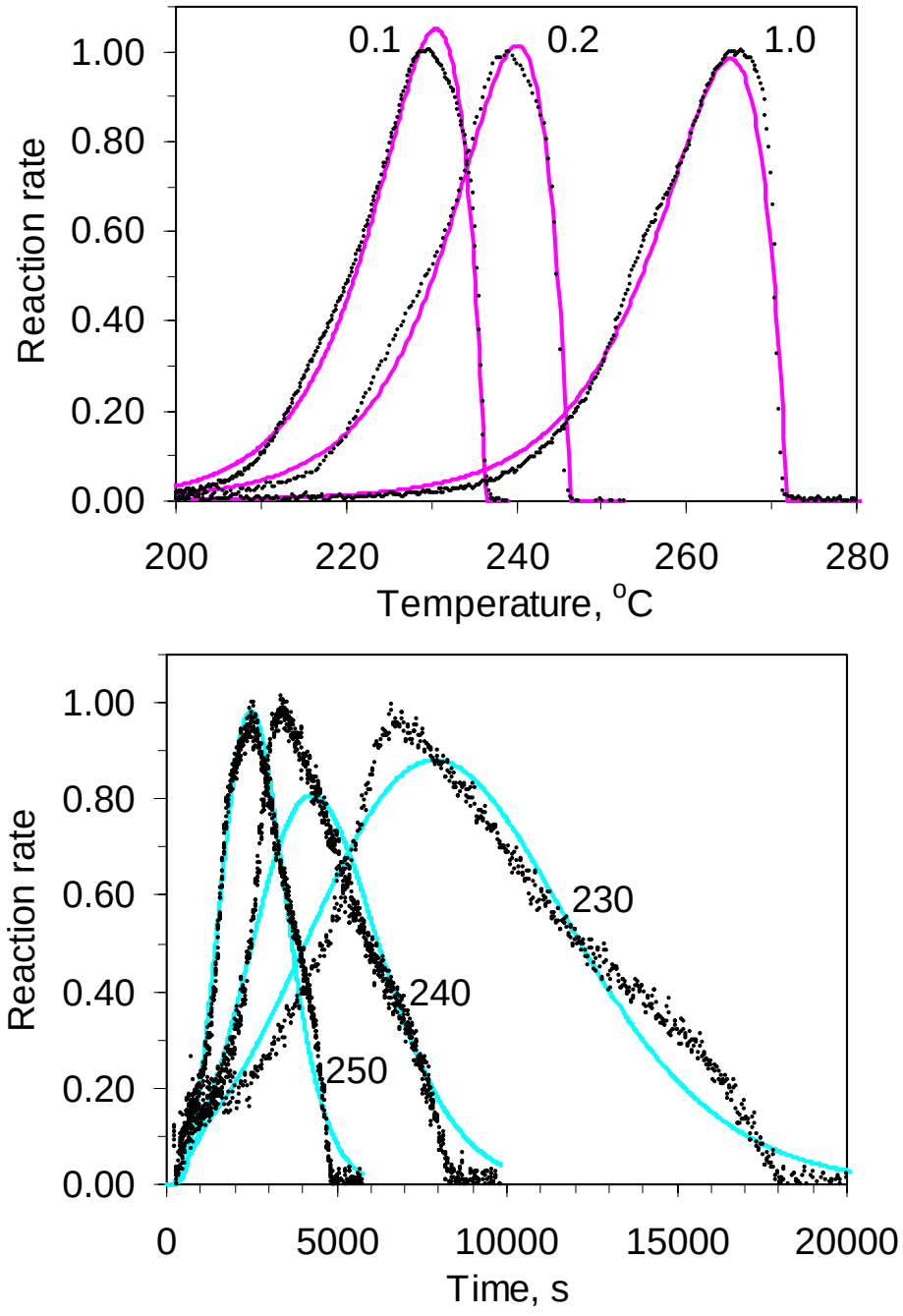

Figure 3. Comparison of the isothermal and constant-heating-rate reaction rates with their respective fits to an extended Prout-Tompkins model. The nonlinear regression analysis simultaneously minimized the squared residuals for both rates and fractions reacted for all experiments of each type.

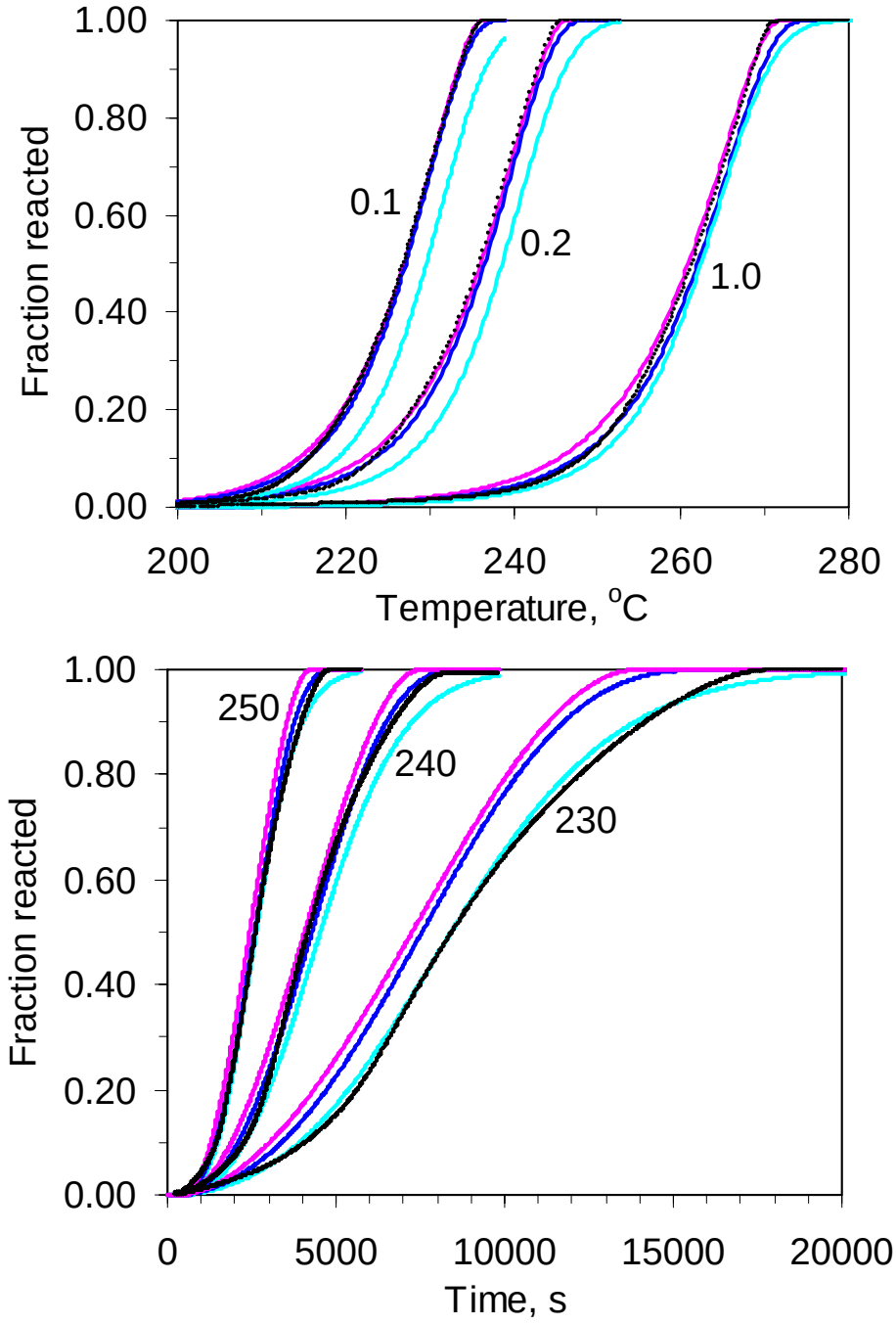

Figure 4. Comparison of all three models to fractions reacted at constant heating rates (top) and constant temperatures (bottom). The red curve is the fit to that the constant heating rate data, the turquoise curve is a fit to the isothermal data, and the blue curve is a fit to both data sets simultaneously.

Subsequent to the original analysis, we collected isothermal TGA data at 210 and 190 ^{o}C to increase the confidence in extrapolation to lower temperatures more typical of storage conditions and thereby obtain more reliable lifetime predictions. Figure 5 compares the measured and calculated fractions reacted for a two component model defined in Table 2. The first component accounts for 2% of the initial mass loss and may well be loss of moisture. The activation energy is noticeably higher than for the 230-250 ^{o}C data, which is reflected in the lag of the calculation compared to experiment for 210-240 ^{o}C. Clearly, the 190 ^{o}C data is largely responsible for the higher activation energy.

Table 2. Summary of kinetic parameters from thermal analysis of HMX sample B-844.

	fraction	A, s^{-1}	E, kJ/mol	m	n
Isothermal TGA	0.02	7.04×10^{7}	101.1	0.00	1.00
(open pan, 190-250 ^{o}C)	0.98	5.84×10^{13}	167.2	0.691	0.823

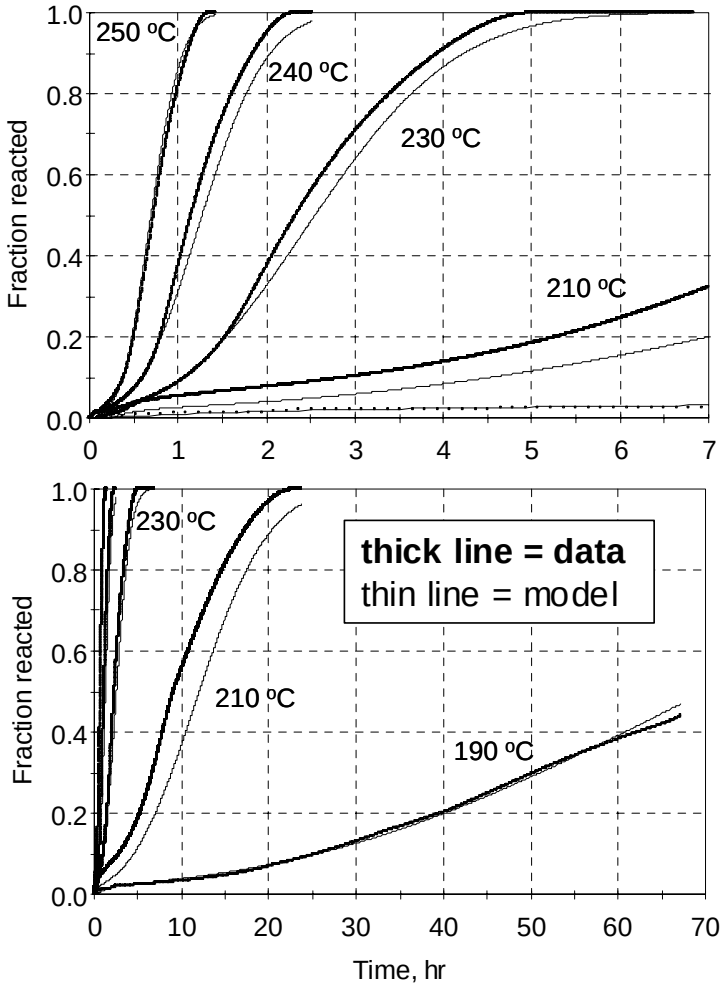

Figure 5. Comparison of model parameters in Table 2 for isothermal weight loss from HMX (open-pan TGA). Two time scales are shown enable a comparison over the entire temperature range. Only partial reaction was achieved at 190 ^{o}C due to the slowness of the reaction.

The results from LLNL can be compared to parameters derived from data supplied by Prof. Chuck Wight at the University of Utah. This data was collected by one of his students, Peter Lofy. Our analysis is given in Table 3. A comparison of isoconversional activation energies provided by Wight to the LLNL Friedman analysis in Figure 6, and a comparison of measured and calculated fractions reacted are given in Figure 7. The calculated temperature for 50% conversion at a heating rate of 0.5 ^{o}C/min is within a few degrees of that in Table 1.

Table 3. Kinetic parameters derived from mass loss for both constant heating rate and isothermal heating of HMX at the University of Utah.

	Constant heating rate			Isothermal		
Friedman	$A_{n=1}$	E	σ_E	$A_{n=1}$	E	σ_E
0.1	5.00E+10	143.1	25.6	1.41E+07	108.3	45.2
0.2	1.51E+14	175.8	14.5	2.53E+11	147.5	26.7
0.3	3.66E+13	167.5	19.6	4.20E+13	168.0	32.7
0.4	3.55E+09	126.5	10.0	4.28E+14	176.9	16.3
0.5	7.18E+07	108.7	6.3	1.43E+12	151.7	14.7
0.6	2.55E+08	113.3	5.9	2.69E+12	153.4	5.4
0.7	7.26E+09	126.9	7.4	3.06E+14	173.4	26.0
0.8	1.94E+11	140.2	9.7	8.85E+13	166.9	8.6
0.9	8.52E+11	144.8	7.5	7.49E+13	164.2	44.5
Kissinger	$A_{n=1}$	E	σ_E	A_{PT}	n	m
(const. h.r. only)	1.347E+09	125.1	7.2	5.135E09	0.900	0.865
Nonlin. Reg. PT	A_{PT}	E	n	m	q	$T_{50\%}$*
const. h. r.	1.495E+11	140.0	0.700	1.068	0.90	247.6
isothermal	6.427E+13	166.6	0.700	0.982	0.90	249.1
both	1.654E+12	151.7	0.700	0.837	0.90	248.3

*Calculated temperature for 50% conversion at 0.5 ^{o}C/min

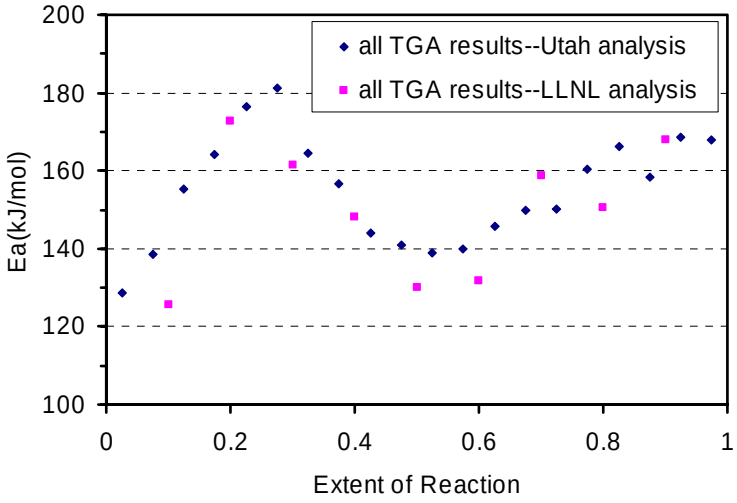

Figure 6. Comparison of isoconversional activation energies by the Utah and LLNL analysis methods. The agreement is very good.

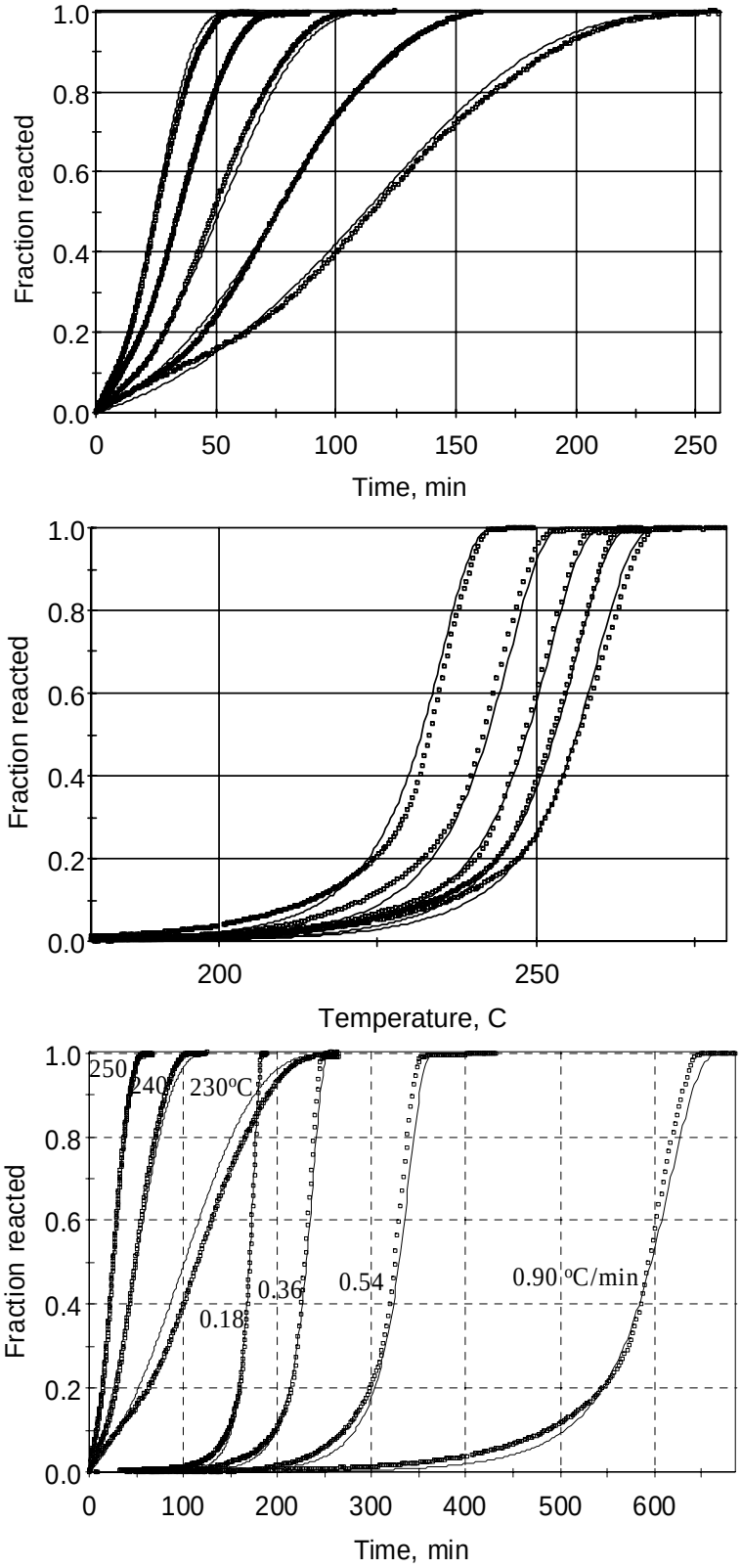

Figure 7. Measured fractions reacted and nonlinear regression fits to an extended PT model for isothermal (230-250 ^{o}C), constant heating rate (0.18-0.9 ^{o}C/min), and both sets simultaneously for HMX mass loss data from the University of Utah.

4.2. Kinetics of heat release from DTA at a constant heating rate

Heat release does not necessarily follow the same kinetics as mass loss, in that they represent different weighted sums of complex processes. The SDT apparatus provides a way of directly comparing how close the two processes are. Of course, the full heat of detonation is not realized in open-pan decomposition, nor is it possible to accurately measure the heat generated in an open-pan DTA experiment. Consequently, for making this comparison, we have normalized the DTA results to match the initial reaction rate curves.

The resulting comparison of mass loss and heat release at three heating rates is shown in Figure 8. The multiple reaction processes noticed in the previous section for mass loss are clearer in the heat release profiles. The low-temperature shoulder is close to the tallest peak at 1 ^{o}C/min. A high-temperature shoulder is also pronounced at 0.2 and 1 ^{o}C/min. At 2.5 ^{o}C/min, the reaction profiles change qualitatively, as was noted in Figure 2. This probably corresponds to thermal runaway or gas-phase ignition.

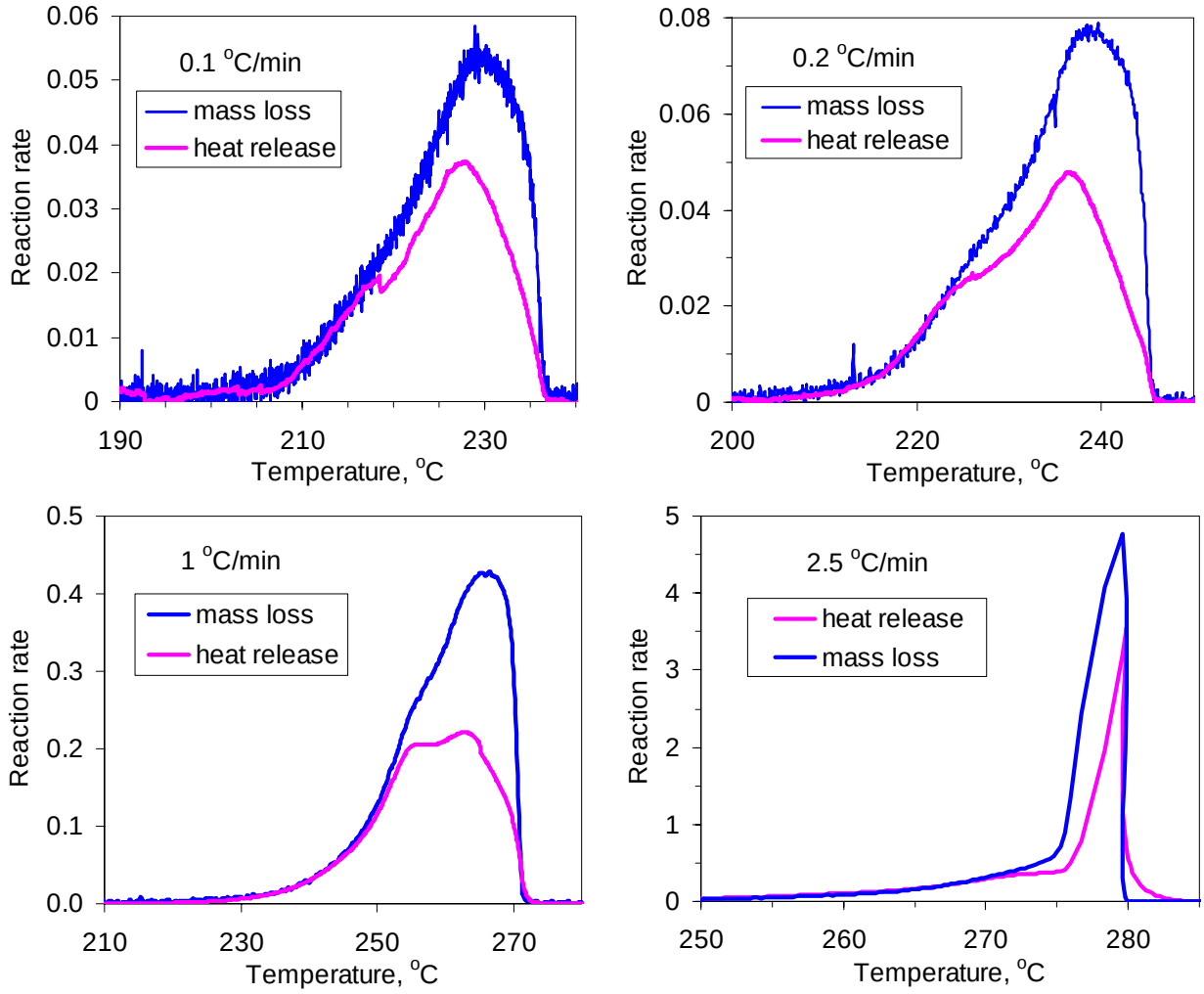

Figure 8. Comparison of heat release and mass loss reaction rates for HMX at four heating rates.

The DTA data was fitted to the various kinetic models as before. Table 4 reports both Friedman and Modified Coats-Redfern isoconversional analysis. The modified Coats-Redern method is base on the integral rather than the rate as for the Friedman method. Figure 9 shows a comparison of measured and calculated reaction curves for single and three-reaction nucleation growth models. Although the three-reaction model provides a qualitative improvement in agreement with some aspects of the data, the overall residual sum of squares are about equal. This lack of improvement is probably due to two factors. First, the single reaction model is truly optimized by the computer program, which the three-reaction model is partially optimized by iteration. Also, the profile shape changes with heating rate, indicating the reaction mechanism is not three independent parallel reactions. Consequently, the low temperature shoulder is overestimated at the low heating rate and underestimated at the high heating rate.

Table 4. Kinetic parameters from HMX DTA data at constant heating rates of 0.1, 0.2, and 1.0 ^{o}C/min.

	Friedman			Modified Coats-Redfern		
Fraction reacted	$A_{n=1}$	E	σ_E	$A_{n=1}$	E	σ_E
0.1	1.29E+09	125.8	9.1	7.92E+09	137.4	7.9
0.2	1.45E+10	134.5	6.7	6.78E+09	134.9	7.5
0.3	1.96E+12	154.6	5.7	1.48E+10	137.1	7.5
0.4	6.43E+11	149.3	1.6	3.29E+10	139.6	6.8
0.5	6.54E+10	139.0	2.0	4.69E+10	140.5	5.7
0.6	1.35E+10	131.4	2.4	4.69E+10	139.9	4.9
0.7	1.73E+10	131.5	3.7	4.23E+10	138.8	4.6
0.8	3.44E+10	133.7	3.5	4.33E+10	138.2	4.4
0.9	9.41E+10	136.9	1.5	5.00E+10	138.0	4.1
Single PT rxn.	A_{PT}	E	n	m		$T_{50\%}$*
	5.957E+10	138.0	0.651	0.523		246.9
Three PT rxns.	A_{PT}	E	n	m	f	242.4
	2.500E+10	127.6	1.00	1.00	0.29	
	9.600E+10	136.0	1.00	0.90	0.49	
	6.300E+10	136.0	1.00	0.50	0.22	

*Calculated temperature for 50% conversion at 0.5 ^{o}C/min

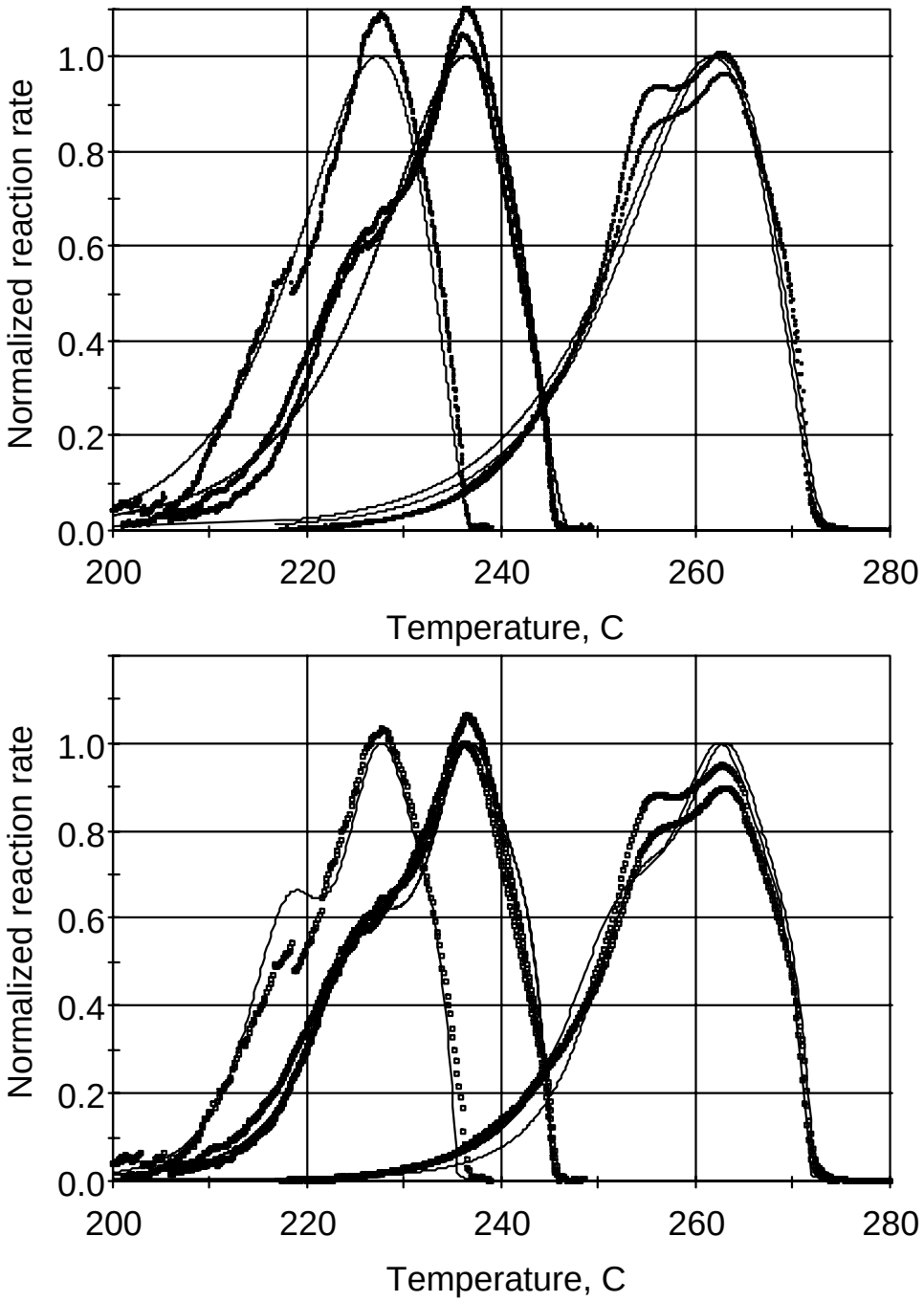

Figure 9. Comparison of LLNL DTA data at 0.1, 0.2, and 1.0 ^{o}C/min with the one- and three-reaction models in Table 4. The residual sum of squares is not improved substantially, because the relative abundance of the three reactions does not appear to be independent of heating rate, so the profile shapes change.

4.2. Kinetics of heat release from isothermal DSC

Differential scanning calorimetry gives more reliable baselines that DTA for estimating reaction rates. Even so, the thermal transients at the beginning of a nominally isothermal experiment do provide a challenge. Our experiments were conducted in the modulated mode, with a peak-to-valley amplitude of 10 ^{o}C and cycle frequency ranging from 1.6/min at 232 ^{o}C to 0.6/min at 251 ^{o}C. Fourier filtering is used to separate the reactive (irreversible) and heat capacity (reversible) components of the heat flow. The filtered irreversible signal, a nonlinear estimation of the baseline, and the net HMX decomposition rate are given in Figure 10. The reaction rate again shows multiple reaction processes, with the final process abruptly dropping to the baseline.

The kinetic parameters derived from this data are given in Table 5. The isoconversional activation energies are more variable and somewhat higher than from other experiments. A comparison of the fit with the data is given in Figure 11. The model fits the profile overall, but it misses a few key aspects. First, the asymptotic approach to baseline is not consistent with the abrupt drop in the experiments. The drop is not as pronounced at 232 ^{o}C, but that may be a baseline correction limitation. Second, the fit tends to miss the sharpness of the initial rise in reaction rate and peaks at longer times for the two higher temperatures.

Figure 12 compares the isothermal DSC data with calculations using the kinetics derived from the constant-heating-rate DTA data. The calculations agree with experiment pretty well at the higher two temperatures, although it misses the change in relative height of the first two peaks from 241 to 251 ^{o}C. However, they are too fast at the lowest temperature. The slowness of the isothermal reaction rate at 230 ^{o}C appears to be a recurring theme.

Table 5. Kinetic parameters from HMX isothermal DSC data at 232, 241, and 251 ^{o}C.

	Friedman			
Fraction reacted	$A_{n=1}$	E	σ_E	
0.1	2.54E+15	187.2	43.9	
0.2	6.79E+09	130.4	22.0	
0.3	4.74E+09	128.2	8.1	
0.4	3.13E+12	155.5	1.9	
0.5	1.25E+15	180.4	4.1	
0.6	1.06E+16	189.0	13.4	
0.7	4.46E+16	194.7	21.6	
0.8	1.13E+18	208.1	29.0	
0.9	1.00E+19	216.6	17.4	
Single PT rxn.*	A_{PT}	E	n	m
	2.324E+12	150.3	1.195	0.850

*Calculated temperature for 50% conversion at 0.5 ^{o}C/min equals 247.9 ^{o}C

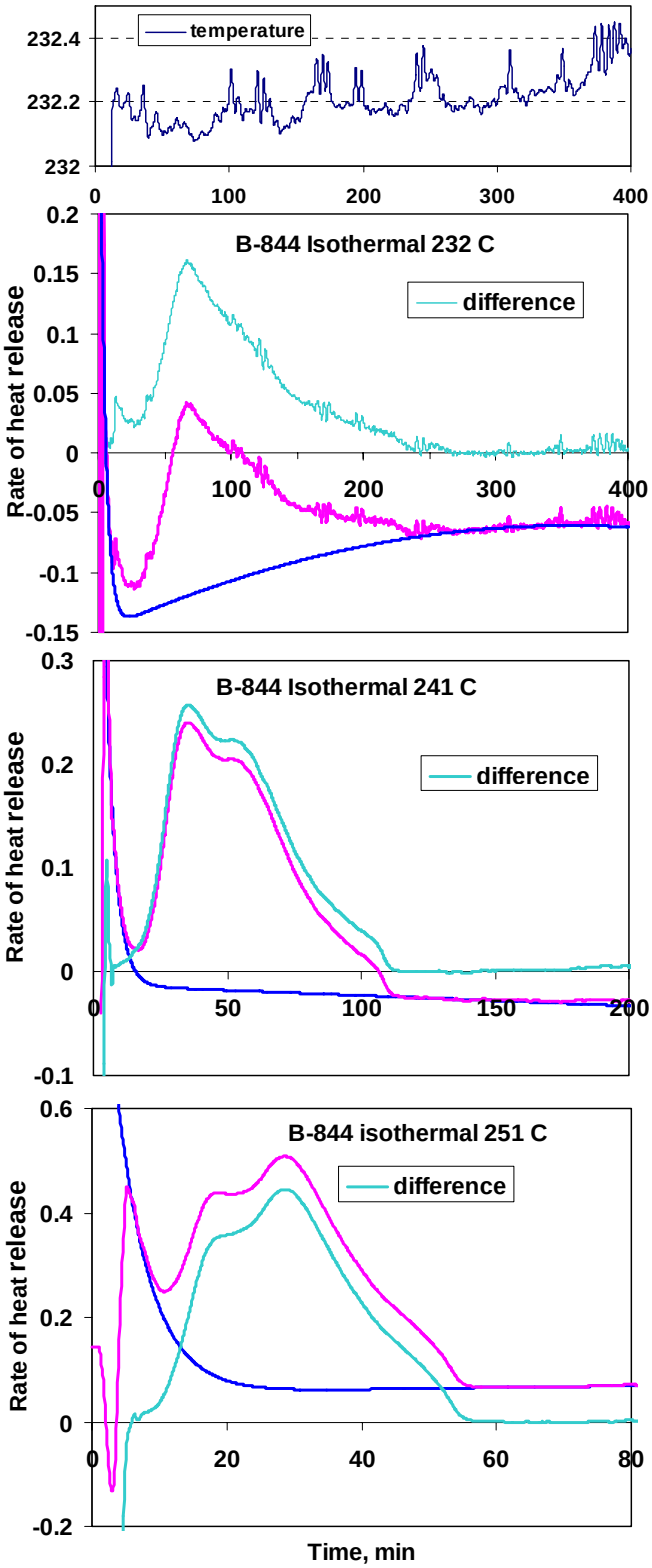

Figure 10. Baseline corrections of isothermal modulated DSC data. The upper figure shows residual spikes in the lowest temperature after Fourier transform, which are also reflected in the rate data.

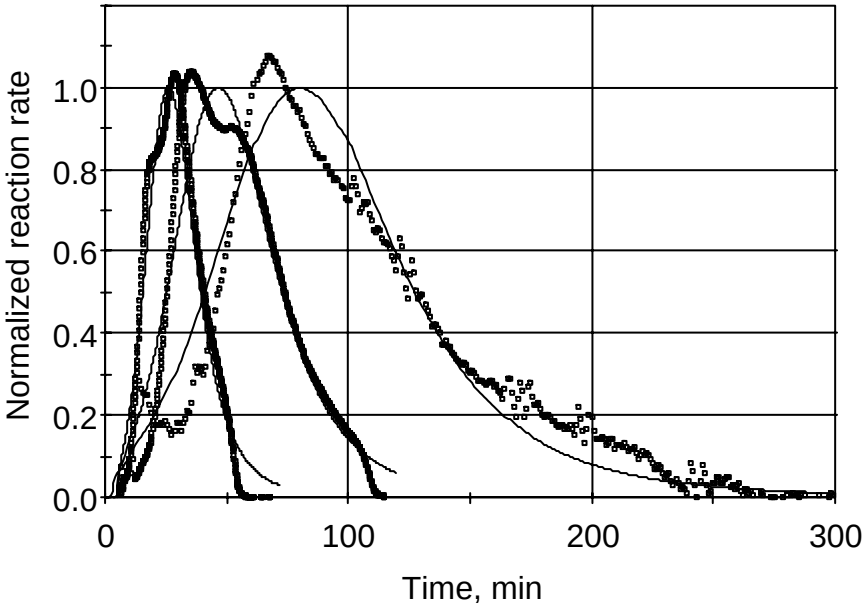

Figure 11. Fit of isothermal open-pan DSC data at 232, 241, and 251 ^{o}C to a nucleation-growth kinetic model.

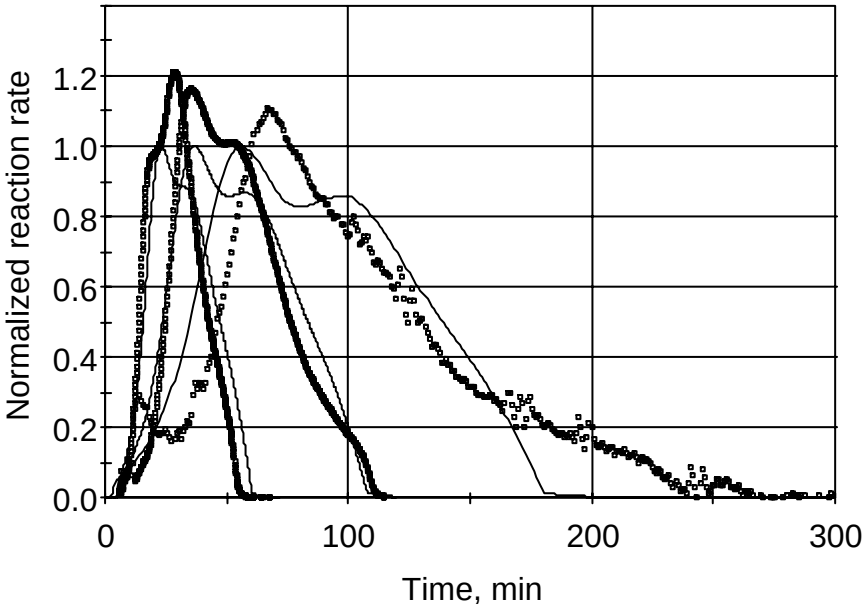

Figure 12. Comparison of the isothermal DSC data with the three-reaction model derived from the DTA data at a constant heating rate.

4.3. Comparison to heat release from University of Utah data

We next compare our results to those from analyzing constant heating rate and isothermal data from the University of Utah. The results are summarized in Table 6, and a comparison of measurements and calculations is shown in Figure 13. Not as much time was spent optimizing these parameters, but they are shown for completeness. The activation energies are similar, but generally higher than we obtained. The reaction profiles show some of the same multi-reaction characteristics. Again, the lowest isothermal reaction rate is slower than expected from fitting both data types simultaneously. Note that the two lowest temperature experiments in Figure 13 (top) appear somewhat incompatible. It is also noteworthy that for a constant heating rate, the heat release kinetics are about 10 ^{o}C slower (higher temperature) than the mass loss kinetics.

4.4. Kinetics of heat release from closed pan experiments

While the open-pan experiments are interesting and useful to learn about decomposition reaction characteristics, applications of high explosives involve confined spaces in which reaction products can undergo secondary reactions with one another. Furthermore, it is well known that the amount of heat release in an open pan is substantially smaller than in a closed or partially closed pan. Consequently, we undertook a study of heat release kinetics in a hermetically sealed pan. Experimental results were variable, and Figure 14 shows the results of all experiments. The experiments in dark blue were deemed to be the most representative.

Table 6. Heat release kinetic parameters derived from both constant heating rate and isothermal heating of HMX at the University of Utah. A reaction order of 1.0 was assumed in all cases.

	Isothermal and const. h.r.			
Friedman	$A_{n=1}$	E	σ_E	
0.1	2.98E+13	171.0	37.9	
0.2	8.32E+11	154.0	37.2	
0.3	6.34E+11	151.9	33.3	
0.4	1.53E+12	155.0	30.3	
0.5	1.45E+12	154.2	30.3	
0.6	5.25E+11	149.3	35.0	
0.7	1.15E+11	142.1	39.8	
0.8	2.54E+10	134.8	38.2	
0.9	3.76E+10	135.3	29.0	
Nonlin. Reg. PT	A_{PT}	E	m	$T_{50\%}$*
const. h. r.	3.315E+14	177.0	0.699	255.5
isothermal	8.387E+12	158.1	0.911	257.0
Both (q=0.90)	2.184E+13	162.7	0.869	257.2

*Calculated temperature for 50% conversion at 0.5 ^{o}C/min

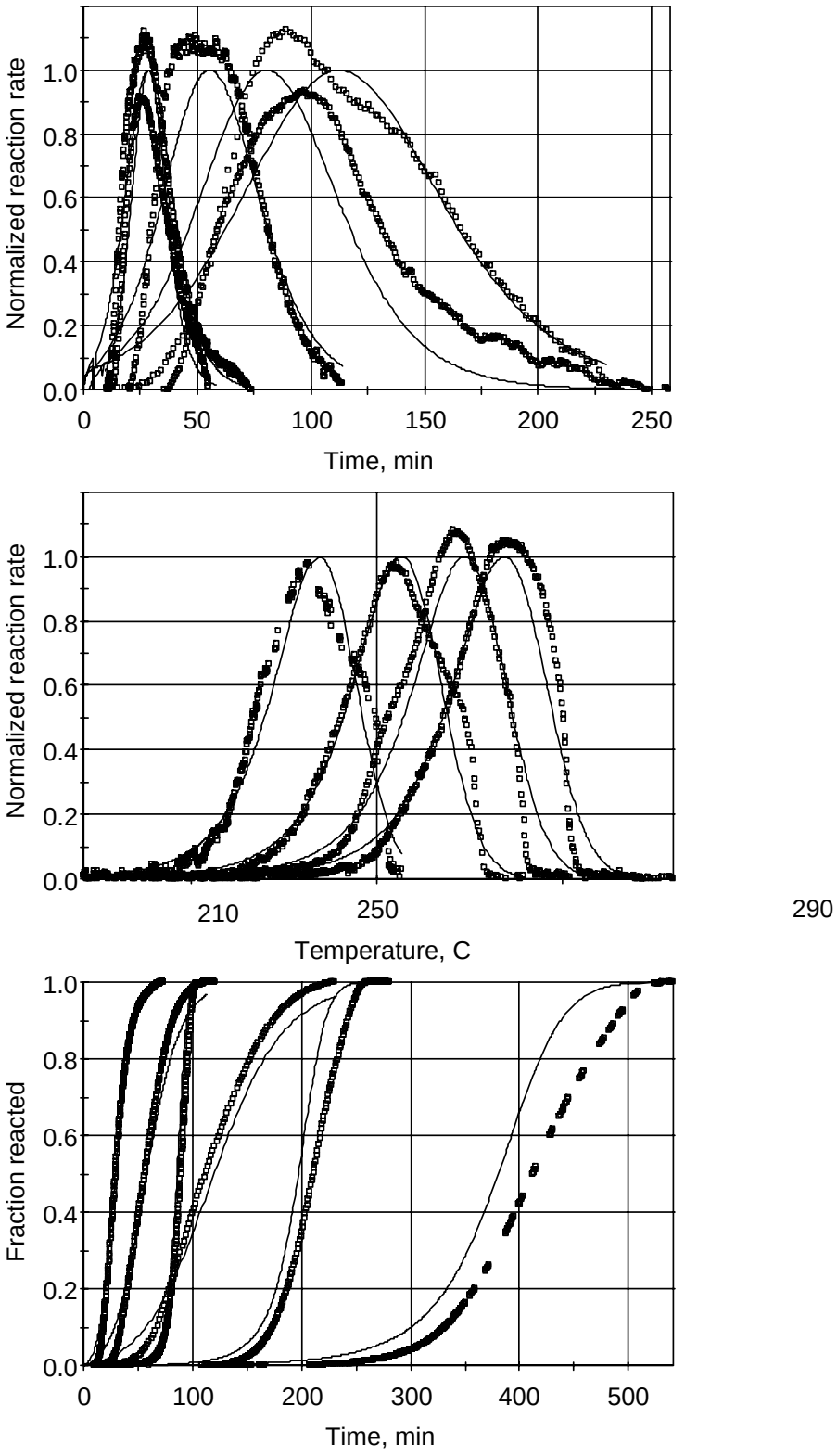

Figure 13. Summary of nucleation-growth model fits to data from University of Utah. Top: isothermal at 235, 242, 247, 257, and 263 ^{o}C. Middle: constant heating rates of 0.1, 0.25, 0.5, and 0.75 C/min. Bottom: simultaneous fit to 235, 245 and 255 ^{o}C and 0.1, 0.25, and 0.75 ^{o}C/min.

The original intent was to fit the difference in open and closed pan experiments to a secondary reaction model, but the secondary reactions actually cause the entire reaction to complete faster, so they are not additive. Comparing to the results in Figure 8, the reaction is completed about 5 ^{o}C sooner at 0.1 ^{o}C/min and 10 ^{o}C sooner at 1 ^{o}C/min. Consequently, we fitted the closed pan experiments to a single reaction model. The results are summarized in Table 7, and a comparison of measured and calculated rates and fractions reacted are given in Figure 15. In addition, a better fit (residual sum of squares about half as large) is accomplished using two parallel nucleation-growth reactions having activation energies fixed at 146.4 and 159.0 kJ/mol (25%:75%).

The activation energies from these experiments are among the highest from any LLNL data set in this report, but they are still within the range of that determined from the Utah data. The highest heating rate data appears to be sharper and shifted to lower temperatures more than the lowest heating rate data, so one concern is that the highest heating rate may be approaching thermal runaway. That would shift the activation energy above its correct value, with a compensating increase in the frequency factor.

An important related observation is that the heats released in these hermetically sealed pans are 42, 38, and 39% of the detonation value (gaseous water product) at 0.1, 0.35, and 1.0 ^{o}C/min, respectively. Even though nominally sealed, the pans do lose mass, and apparently the gases escape before they completely react. This may not be a problem when using these kinetic parameters to predict such quantities such as the time to explosion, where the reaction conditions are mild until the explosion occurs. However, one may need to use the lower energy released for such calculations to property calculate the time to explosion.

Table 7. Kinetic parameters derived from constant heating rate of HMX in a hermetically sealed vessel at LLNL.

	Constant heating rate					
Friedman	$A_{n=1}$	E	σ_E			
0.1	1.30E+10	136.4	0.5			
0.2	1.53E+12	154.8	11.7			
0.3	4.68E+13	167.9	12.9			
0.4	1.56E+14	171.7	6.8			
0.5	5.40E+14	175.8	3.4			
0.6	1.37E+15	178.4	12.0			
0.7	5.56E+15	182.8	19.1			
0.8	8.44E+16	192.7	19.9			
0.9	1.42E+19	212.3	20.6			
Kissinger	$A_{n=1}$	E	σ_E	A_{PT}	n	m
(c.h.r. only)	2.06E+12	156.1	31.7	8.678E+12	0.402	0.900
Nonlin. Reg. PT	A_{PT}	E	n	m	$T_{50\%}$*	
const. h. r.	3.806E+13	164.4	0.320	0.635	250.0	

*Calculated temperature for 50% conversion at 0.5 ^{o}C/min

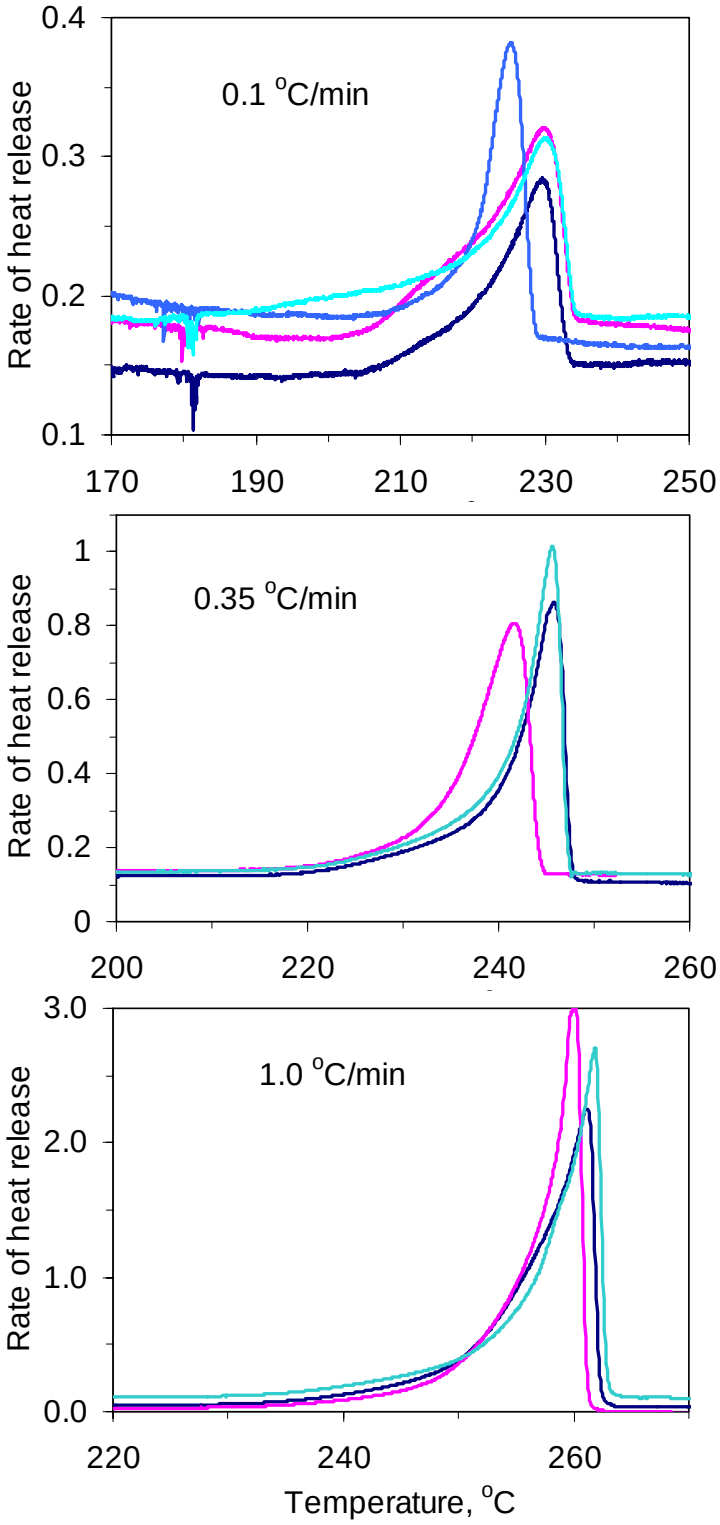

Figure 14. Replicate measurements of heat release for HMX heated at constant rates in a hermetically sealed vessel. The dark blue experiment in each case was selected for kinetic fitting.

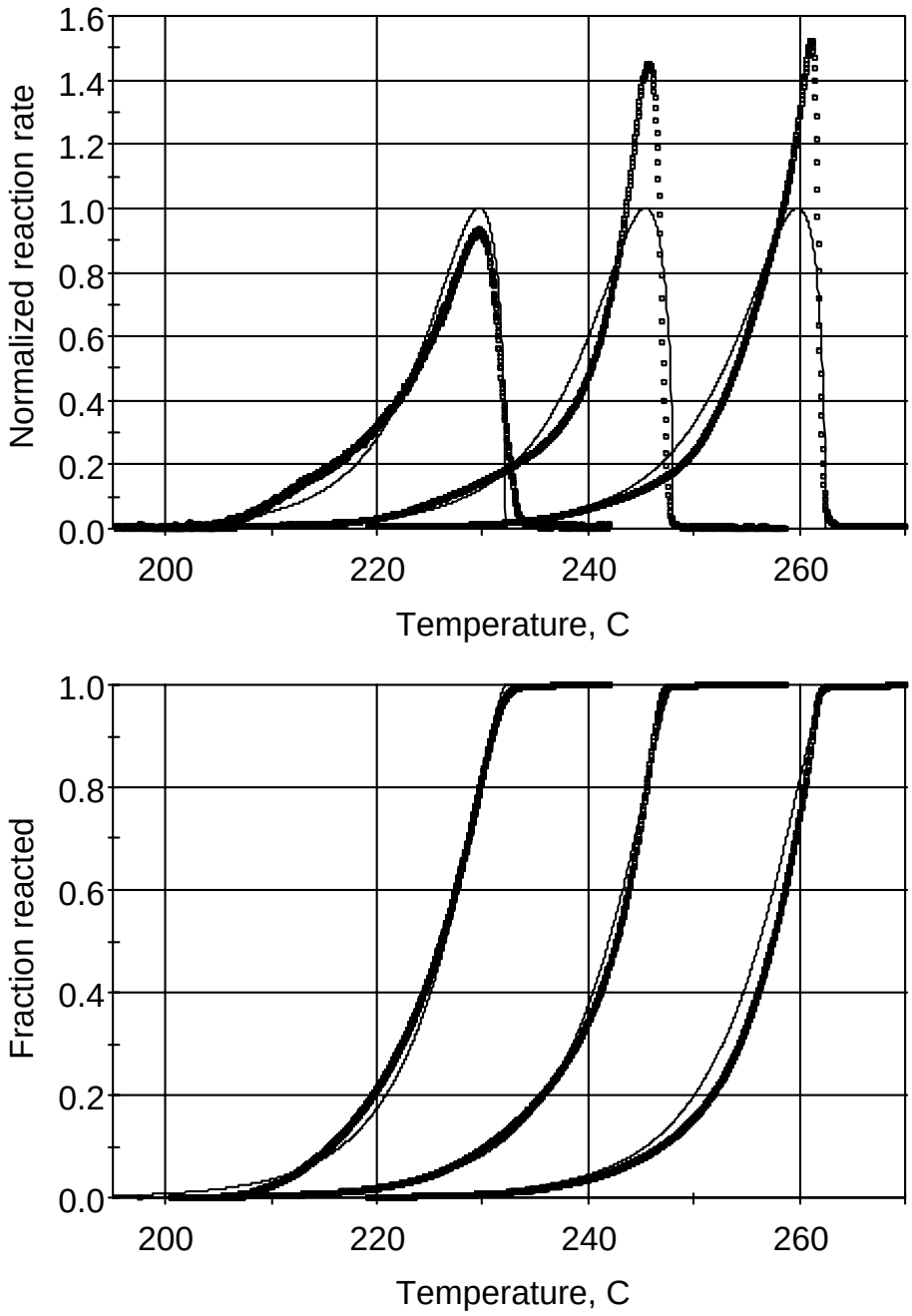

Figure 15. Comparison heat release from heat release from HMX at 0.1, 0.35, and 1.0 ^{o}C/min in a sealed pan with a fit to a single nucleation-growth model: rate (top) and fraction reacted (bottom).

5. Other Estimates of the Global Activation Energy

Kinetic data from this report can be combined with other measurements in the literature to obtain an average activation energy using a different approach. Figure 16 shows an Arrhenius plot at 10% decomposition for four distinctly different data sets—two from LLNL and two from Sandia National Laboratories (SNL). These four data sets fall on a remarkably smooth trend. We showed earlier in this report that the LLNL and University of Utah data sets agree well, so they would also follow the same trend line.

The reaction rate increases by six orders of magnitude from 120 to 260 °C. The line corresponds to an activation energy of 165.1 kJ/mol, which lies within the range of the activation energies from the LLNL and Utah data. The isothermal gas release experiments of Behrens [2] have a higher slope consistent with an activation energy of about 210 kJ/mol. Furthermore, additional experiments by Andrzjewski [3] at 100 and 80 °C, having decomposition extents on the order of 1% and 0.1% suggest a lower activation energy of ~96 kJ/mol, although deriving an activation energy in this manner violates the isoconversional principle.

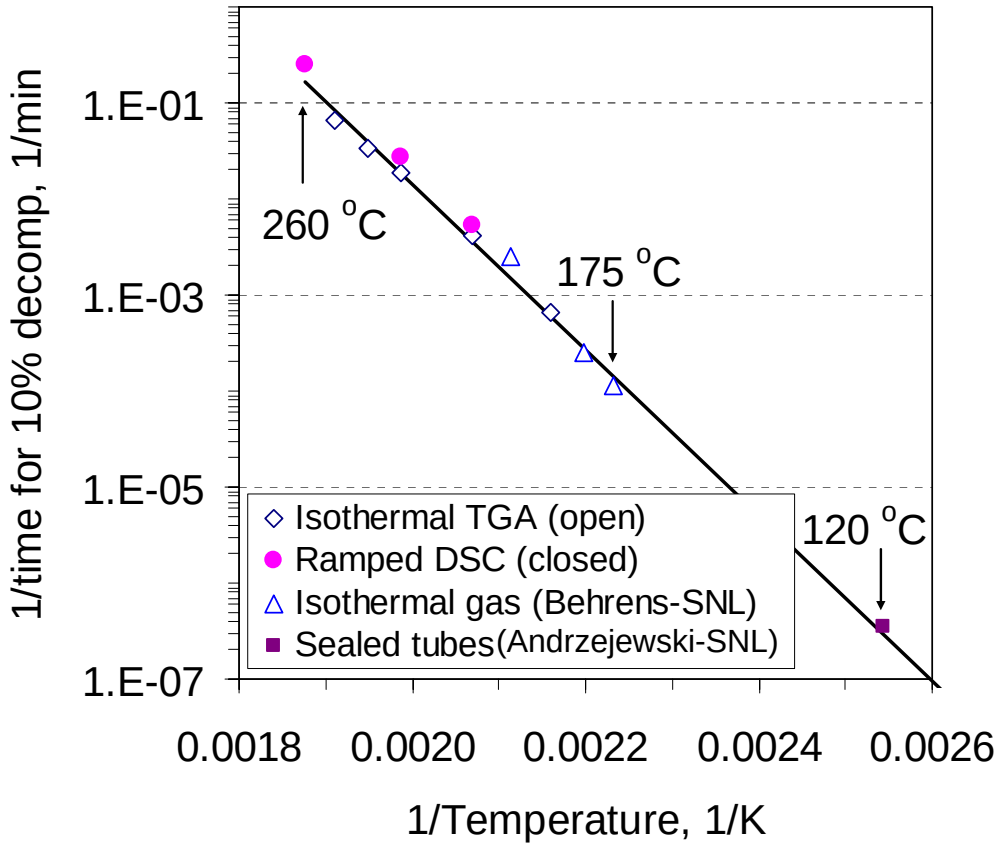

Figure 16. Arrhenius plot at 10% conversion of HMX decomposition rates measured by four distinct methods over a very wide range of temperature, indicating an average activation energy of 165 kJ/mol.

Our interpretation of these differences is that any set of data limited in terms of reaction extent or temperature is prone to errors (statistical, systematic experimental, or mechanistic) that can skew the activation energy even though the overall rate constants are approximately correct. By compiling a greater number of experiments spanning a wider set of conditions and temperatures, these fluctuations can be put in their proper perspective. While the differences between open and closed systems are real, they are only of order 2x, which is small from this perspective. Consequently, we conclude that the mean activation energy of HMX decomposition is most likely in the 165 kJ/mol range.

6. Conclusions

A broad range of experiments and kinetic analysis methods, both at LLNL and at the University of Utah, indicates that the global activation energy is in the vicinity of 150 kJ/mol, depending on conditions, which is lower than determined by most workers. The activation energies from LLNL data tend to be slightly lower than from the Utah data. The activation energies from these two sets of thermal analysis data are lower than the general published literature. They result from more careful attention to using conditions in which sample self-heating is minimized, meaning sample sizes less than 0.5 mg and pyrolysis temperatures lower than about 260 ^{o}C. At higher temperatures, both thermal runaway and interference of the melting endotherm prevent getting accurate thermal histories.

The reaction in an open pan shows evidence for three global processes, although constant heating rate mass loss is described fairly well by a single nucleation-growth model. The activation energies determined by model fitting to multiple thermal histories are similar to those determined by isoconversional analysis.

The decomposition reaction is accelerated in a sealed pan, presumably because gaseous intermediates react with the decomposing solid. The heat release in a closed pan completes 5-10 ^{o}C sooner that either heat release or mass loss in an open pan. A single nucleation-growth model fits the heat release from the sealed pan (~40% of the detonation value) fairly well, and its use is preferable for cases in which a simple model is needed to predict high explosives performance.

Additional consideration of lower temperature decomposition data from SNL produces an excellent Arrhenius relationship with an activation energy of ~165 kJ/mol, which is well with the range of values from the more limited temperature range data from LLNL and the University of Utah.

7. Acknowledgments

We thank Professor Charles Wight of the University of Utah and W. J. Andrzejewski of Sandia for supplying us with some of their groups' unpublished data for our comparison of methods and Frank Garcia and Kevin Vandersaal for supplying samples.

8. References

[1] S. Vyazovkin, C. A. Wight, Ann. Rev. Phys. Chem. 48 (1997) 119.
[2] R. Behrens and S. Bulusu, in *Decomposition, Combustion, and Detonation Chemistry of Energetic Materials*, MRS Symp. Proc. 418, T. Brill et al., Eds., Materials Research Society, Pittsburgh, PA.1996, pp. 119-128.
[3] A. K. Burnham, R. K. Weese, and W. J. Andrzejewski, "Kinetics of HMX and CP Decomposition and Their Extrapolation for Lifetime Assessment," LLNL Report UCRL-TR-xxxxxx (Nov., 2004).
[4] A. K. Burnham and R. L. Braun, Energy & Fuels 13 (1999) 1.
[5] Friedman, H. L. J. Polymer Sci., Part C. 6 (1963) 183.
[6] A. K. Burnham, J. Therm. Anal. Cal. 60 (2000) 895.
[7] H. E. Kissinger, Anal. Chem. 29 (1957) 1702.